

An inverse approach in obtaining shape functions for a superconvergent thin plate element

S. Faroughi^{a*} and H. Ahmadian^b

^aFaculty of Mechanical Engineering, Urmia University of Technology, Urmia, Iran; ^bSchool of Mechanical Engineering, Iran University of Science and Technology, Tehran, Iran

(Received 2 January 2014; final version received 28 June 2015)

This article presents an inverse approach to provide shape functions associate with a superconvergent thin plate element formulation. In the proposed approach, candidates for shape functions of an element are selected using a series of functions such as, trigonometric series, simple and hierarchical polynomials or a combination of them. Next, one imposes all the physical, geometrical, compatibility and completeness constraints associated with the concerned element on these function. In the final stage, the unknown parameters of the shape functions are determined by minimizing the discrimination errors in the element formulation. The proposed method is employed to determine the shape functions associate with the superconvergent plate element formulation. The accuracy of the obtained formulation is examined against previously developed plate models using several numerical examples. These comparisons indicate the developed model provides more accurate results both in local and global coordinates system.

Keywords: shape functions; thin Kirchhoff plate; hierarchal polynomials; inverse approach; superconvergent formulation

1. Introduction

In classical finite element (FE) method, two general approaches, so-called h version and p version, are used to improve the accuracy of model and its rate of convergence. In h version, the order of element shape functions is kept fixed, while the number of elements is increased in such a way that maximum size of the elements, i.e. h , approaches to zero.[1] On the other hand in p version, the element size remains constant while the order of the interpolation functions is progressively increased until the desired rate of convergence is achieved.[2] There are several admissible models reported in the literature for rod, beam and plate elements based on either of h or p approaches such as polynomial shape functions,[3–10] spline wavelet shape functions [11–14] and Fourier p-element.[15]

Employment of an inverse approach is another method to provide an accurate FE model. In this approach, an accurate element formulation is derived by minimizing the discretization errors in a parametric element model. Discretization errors arising from replacing a continuous media by one composed of FEs. An optimum element

*Corresponding author. Email: shirko@just.ac.ir

formulation is normally referred to a formulation which leads to results with superconvergent properties. The inverse approach was introduced by Argyris et al. [16], Bergan et al. [17], and Simo and Rafai [18] to enforce constraints on the stiffness formulation and guarantee the element model passing the patch test. MacNeal [19], Kim [20], Hanssan [21] and Fried et al. [22,23] obtained superconvergent models by eigenvalue convergence analysis for rod, beam and membrane elements in a local coordinate. Stavrinidis et al. [24] and Ahmadian et al. [25] derived superconvergent element formulations by minimizing the discretization errors for several elements. Ahmadian et al. [26] derived the superconvergent mass matrix for thin plate element by minimizing the bias error in adjacent nodes. Furthermore, Faroughi [27] developed the superconvergent formulation for beam element with lateral displacements as sole degrees of freedom (DOF). In all aforementioned cited papers,[16–27] the superconvergent formulations are obtained in local coordinate systems without using shape functions. The absence of shape functions in element formulation is the drawback of the inverse method owing to the fact that the formulation cannot be transformed using these functions from local to global coordinates. Therefore, this restricts the use of the superconvergent models to be applied in modelling practical structures.

In the literature, there are few contributions in order to find shape functions associated with the superconvergent element models. Kim [20] developed a method to find shape functions of superconvergent rod element using a linear combination of shape functions related to lumped and consistent models. The mentioned method cannot be applied for elements possessing rotation as DOF as the superconvergent mass matrix of these elements cannot be established using a linear combination of lumped and consistent models.[24] Further, Ahmadian et al. [28,29] proposed a method to obtain shape functions of superconvergent mass matrices using a series of trigonometric functions. They obtained the shape functions associated with superconvergent rod, beam and transverse vibration membrane elements. Recently, Faroughi et al. [30] developed a method to obtain shape functions associated with superconvergent stiffness matrix (SCSM) of membrane element using hierarchical polynomials which have been employed as shape functions of transverse vibrating membrane,[31] and plate [32,33] elements. Beslin et al. [34] used hierarchical trigonometric shape functions for predicting high-order modes of bending plate.

Ahmadian et al. [25] obtained the SCSM of thin plate element using inverse method. They showed that the accuracy of the obtained stiffness matrix is of 4th order, $O(h^4)$, while the accuracy of the other models documented in the literature is of order two. Despite its superiority in convergence, the model suffers from lack of displacement function, i.e. there are no shape functions corresponding to the SCSM. This prevents one to transform the element from local to global coordinates using the existing methods. The goal of this article was to obtain the shape functions associated with SCSM of thin Kirchhoff plate element. In order to form the shape functions of this SCSM, the hierarchical polynomials are added to the classical shape functions of thin plate element. The hierarchical polynomial employed in the present work includes some unattributed coefficients. These coefficients are determined such that the corresponding shape functions satisfy the general requirements of compatibility, completeness, physical constraints and finally regenerating the superconvergent element formulation.

The hierarchical FE method is successfully applied to vibration and buckling problems of plates and shells.[35] Legendre orthogonal polynomials and trigonometric

functions have been used as the hierarchical shape functions. Bardell was the first who carried out early researches about applying the hierarchical FE to investigate the vibration flat and skew plate. For instance, he studied vibration problems of thin cylindrical shell panels using K-orthogonal polynomials satisfying both displacement and slope continuity (C^1 continuity) in [32]. Further, Barrette et al. [36] studied the vibration of stiffened plates using hierarchical trigonometric functions and Beslin et al. [34] investigated a hierarchical functions set for predicting very high-order plate bending modes. Houmat [31] also used hierarchical FE analysis for vibration of membranes. The complementary hierarchical polynomials are used in this study to improve the strain field of the element, resulting accurate modelling of strain energy and fast eigen convergence of the model.

The outline of the article is as follows: Section 2 presents the algorithm to obtain the shape functions associated with superconvergent formulation. In Section 3, the development of shape functions for SCSM of thin plate element is described. Section 4 investigates the convergence rates of the SCSM in local and global coordinate systems followed by concluding remarks in Section 5.

2. General algorithm to describe the shape functions

In classical FE, shape functions of an element are supposed to have unknown coefficients, which are determined by different methods such as assigning a unite displacement to one DOF while other DOF has zero displacements. Here, a new method is proposed to obtain shape functions. In this method, shape functions are inversely obtained by maximizing the eigen solution convergence of associated mass and stiffness matrices. In order to inversely generate the shape functions, the following procedure should be taken.

Consider an element with n DOF and n shape functions. Initially, one selects n functions such as simple polynomials from Pascal triangle, trigonometric series, hierarchical polynomials, etc. These functions with their unknown coefficients are considered as candidate shape functions for the element. Next, the following constraints are imposed to the selected functions in order to obtain shape functions of element.

- (1) The value of each shape function should be equal to unity on its associated DOF and equal to zero on the other DOF.
- (2) Edge modes nonzero along one edge and zero at all other edges and vertices. Thus, it postulates that edges have a magnitude of zero over any boundary of the element (a side in 2D, a face in 3D), which does not include node i .
- (3) Each shape function has interelements compatibility and degrees of continuity (C^0 , C^1 , ...) and also satisfies completeness conditions.
- (4) Moreover, the shape functions must satisfy the physical constraint of the element. These physical requirements are related to the geometry of elements, including axes of symmetry of the element, rigid body, etc.

The first three conditions are extensively explained in the literature, but the last condition requires further explanation. In order to better understand the physical requirement, consider a two-node rod element with unit length, as an example. Each node has one DOF as shown in Figure 1. The rod element has one axis of symmetry

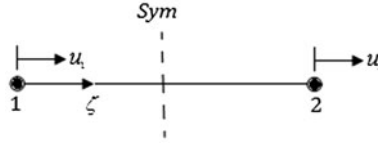


Figure 1. The geometry of rod element.

and one rigid body mode. If the rod element is rotated 180° about the axis of symmetry, the geometry of rod element will remain constant, but the positions of nodes 1 and 2 will be exchanged. Therefore, this behaviour must be reflected by shape functions which are formulated as follows

$$N_2(\zeta) = N_1(1 - \zeta) \quad (1)$$

Here, ζ is natural coordinates of the element. Indeed, the calculated shape functions should be able to generate the rigid body modes of the element. It means the calculated shape functions must represent the deformed shape of element compatible with rigid body requirements. Here, for a rod element having one rigid body mode, this requirement leads to

$$N_1(\zeta) + N_2(\zeta) = 1 \rightarrow N_2(\zeta) = 1 - N_1(\zeta) \quad (2)$$

After applying physical constraints, the independent shape functions for each element will be determined. At the final stage, the independent shape functions must reproduce the entries superconvergent formulation defined by the inverse approach. Therefore, the number of equations required to find these unknown coefficients will be determined by employing all the mentioned requirements which are needed to be satisfied.

In the following section, shape functions of a two-dimensional plate element are obtained by enforcing all the geometrical and physical constraints on truncated hierarchical polynomials.

3. Rectangular thin plate element

Here, a four-node rectangular plate element with dimension, $a \times b \times t$ is considered as shown in Figure 2. The element has three DOF at each node. In the literature, there were several formulations for thin plate elements such as MZC,[8,34] BFS,[37] ZQC [38] and recently JWU [39] which are developed based on the minimization of energy functional and virtual work, respectively. The accuracy of these models is of second order, $O(h^2)$.

As mentioned earlier, Ahmadian et al. [25] used the inverse approach to develop a superconvergent formulation for rectangular plate element. The accuracy of the mentioned model is up to fourth order. So far, there is no study addressing shape functions associated with this model, which is the object in this study. Towards this goal, one may employ two-dimensional hierarchical polynomial functions and complementary terms defined based on hierarchical functions to obtain the shape functions of the superconvergent plate element considering the following steps. The complementary terms improve

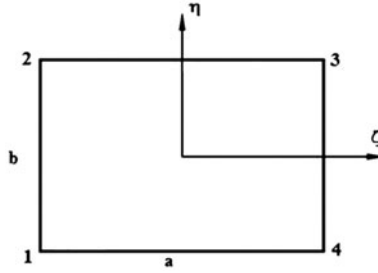


Figure 2. The geometry of rectangular thin plate element.

the strain field of the element, resulting accurate modelling of strain energy and fast eigen convergence of the model.

First one needs to define the displacement field of the plate element using two-dimensional hierarchal polynomial functions as follows:

$$w(\zeta, \eta) = N_1(\zeta, \eta)w_1 + N_2(\zeta, \eta)\theta_2 + N_3(\zeta, \eta)\theta_3 + \cdots + N_{12}(\zeta, \eta)\theta_{12} \quad (3)$$

where N_i , $i = 1, \dots, 12$ are the shape functions of plate element, and w_i and θ_i are the displacement and rotation DOF, respectively. ζ and η denote natural coordinates of elements as shown in Figure 2. Thereafter, twelve functions are selected as candidates for shape functions of the superconvergent element. In the second step, one may impose the physical constraints, to determine the independent shape functions. This particular element has three rigid body modes [25] as follows:

$$\Phi_R = \begin{bmatrix} 1 \\ 1/2 - \zeta \\ \eta - 1/2 \end{bmatrix} \quad (4)$$

The displacement field of Equation (3) must generate the rigid body modes of Equation (4); this imposes the following requirements on the shape functions of the plate element. The first rigid body modes, $w(\zeta, \eta) = 1$, requires all $w_i = 1$, $i = 1, 4, 7, 10$ and $\theta_i = 0$, $i = 2, 3, 5, 6, 8, 9, 11, 12$. Imposing these requirements on displacement field of (3) leads to

$$N_1(\zeta, \eta) + N_4(\zeta, \eta) + N_7(\zeta, \eta) + N_{10}(\zeta, \eta) = 1 \quad (5)$$

In a similar manner, one may calculate the nodal displacements in other two rigid body modes and obtain the following requirements by introducing these nodal variables to the displacement field of Equation (3):

$$-\frac{1}{2}N_1(\zeta, \eta) + N_2(\zeta, \eta) + \frac{1}{2}N_4(\zeta, \eta) + N_5(\zeta, \eta) + \frac{1}{2}N_7(\zeta, \eta) + N_8(\zeta, \eta) - \frac{1}{2}N_{10}(\zeta, \eta) + N_{11}(\zeta, \eta) = \eta - \frac{1}{2} \quad (6)$$

$$-\frac{1}{2}N_1(\zeta, \eta) + N_2(\zeta, \eta) - \frac{1}{2}N_4(\zeta, \eta) + N_5(\zeta, \eta) + \frac{1}{2}N_7(\zeta, \eta) + N_8(\zeta, \eta) + \frac{1}{2}N_{10}(\zeta, \eta) + N_{11}(\zeta, \eta) = \frac{1}{2} - \zeta \quad (7)$$

Another physical requirement is arising from the axes of symmetry of the element. As depicted in Figure 2, the considered element has two axes of symmetry. When the element is rotated by 180° about ζ or η axes, the geometry of the element remains the same; however, nodes 1, 4 and 1, 2 replaced, respectively, by nodes 2, 3 and nodes 3, 4. If the element is rotated 90° about an axis normal to the plate, the aspect ratio of the element will be changed, and consequently, the shape functions corresponding to the rotation DOF are interchanged. Therefore, by employing these symmetry properties on shape functions, twelve shape functions of the plate element can be recast by two independent shape functions as reported in Table 1.

The two independent shape functions of the plate element are selected in the form of following:

$$N_1(\zeta, \eta) = f_1(\zeta, \eta) + \sum_{i=0}^N F_i(\zeta, \eta) \quad (8-a)$$

$$N_2(\zeta, \eta) = g_1(\zeta, \eta) + \sum_{i=0}^N G_i(\zeta, \eta) \quad (8-b)$$

The first part of Equations (8-a) and (8-b), i.e. $f_1(\zeta, \eta)$ and $g_1(\zeta, \eta)$, satisfies the element boundary conditions and are adopted from the classical plate element model shape functions, MZC.[8]

$$f_1(\zeta, \eta) = 1 - \zeta\eta - (3 - 2\zeta)\zeta^2(1 - \eta) - (1 - \zeta)(3 - 2\eta)\eta^2 \quad (9)$$

$$g_1(\zeta, \eta) = (1 - \zeta)\eta(1 - \eta)^2 \quad (10)$$

The N complementary terms of shape functions $F_i(\zeta, \eta)$ and $G_i(\zeta, \eta)$, $i = 0, \dots, N$, are defined based on hierarchal functions, which are described using integrated Legendre polynomials. Zhu [40] primarily presented the polynomial set, and Bardell [32,41] used them to predict natural flexural vibrations of rectangular plates and skew plates. Zhu [40] introduced the polynomial set as:

$$P_m^s(\zeta) = \sum_{n=0}^{m/2} \frac{(-1)^n (2m - 2n - 2s - 1)!!}{2^n n! (m - 2n)!} \zeta^{m-2n} \quad (11)$$

where ζ is the natural coordinate of the element, n is a counter, m is the polynomial degree, $m!! = m(m-2) \cdots (2 \text{ or } 1)$, $0!! = 1$, and $m/2$ denotes the integer part of this product.[32] Equation (11) can be used as hierarchal shape functions with C^{s-1} continuity.[34] Since shape functions of the plate element have C^1 continuity; the value of s in

Table 1. The relationship between twelve shape functions of plate element.

Rotation about normal axis	Rotation about X, Y	Rotation about X, Y
$N_1(\xi, \eta)$	$N_2(\xi, \eta)$	$N_3(\xi, \eta) = -N_2(\eta, \xi)$
$N_4(\xi, \eta) = N_1(\xi, 1 - \eta)$	$N_5(\xi, \eta) = -N_2(\xi, 1 - \eta)$	$N_6(\xi, \eta) = -N_2(1 - \eta, \xi)$
$N_7(\xi, \eta) = N_1(1 - \xi, 1 - \eta)$	$N_8(\xi, \eta) = -N_2(1 - \xi, 1 - \eta)$	$N_9(\xi, \eta) = N_2(1 - \eta, 1 - \xi)$
$N_{10}(\xi, \eta) = N_1(1 - \xi, \eta)$	$N_{11}(\xi, \eta) = N_2(1 - \xi, \eta)$	$N_{12}(\xi, \eta) = N_2(\eta, 1 - \xi)$

$P_m^s(\zeta)$ is set to two. Therefore, Equation (11) can be rewritten as follow for element which local coordinate fall in the interval from 0 to 1:

$$P_{m=r-1}^{s=2}(\zeta) = \sum_{n=0}^{(r-1)/2} \frac{(-1)^2 (2r-2n-7)!!}{2^n n! (r-2n)!} (2\zeta-1)^{r-2n-1} \quad r > 4 \quad (12)$$

Here, r is equal to $m+1$. Table 2 reports these functions for orders of polynomial corresponding to $5 < r < 7$ in which it is noticeable that the polynomials sets have zero displacement and slopes at element nodes.

For two-dimensional, 2D, elements, hierarchal functions are constructed by multiplications of two 1D functions defined in Equation (12). Therefore, the complementary terms of Equation (8) can be described as follows:

$$\begin{aligned} F_i(\zeta, \eta) &= P_{m=r-1}^{s=2}(\zeta) P_{m=r-1}^{s=2}(\eta) \\ G_i(\zeta, \eta) &= P_{m=r-1}^{s=2}(\zeta) P_{m=r-1}^{s=2}(\eta) \end{aligned} \quad (13)$$

The complementary terms in the first shape function, N_1 , must be odd functions, because of anti-symmetric deformation $w(\zeta, \eta)$ with respect to the element's natural coordinates. In other words, the element has two axes of symmetry and an applied displacement at one node, whereas other nodes are fixed, which leads to an anti-symmetric deformation $w(\zeta, \eta)$ with respect to the natural coordinate of the element. As a result, the selected form for the shape function, N_1 , should reflect this fact. However, the complementary terms in the second shape function, N_2 , include both odd and even terms because there is no constraint on deformation $\theta(\zeta, \eta)$ with respect to the element's natural coordinates. Therefore, by substituting the Equations (9), (10), (12) and (13) into Equations (8-a) and (8-b), the selected shape functions are presented as follows:

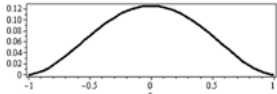
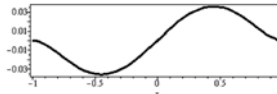

$$\begin{aligned} N_1(\zeta, \eta) &= f_1(\zeta, \eta) + \sum_{r,t=5}^N F_i(\zeta, \eta) = 1 - \zeta\eta - (3 - 2\zeta)\zeta^2(1 - \eta) - (1 - \zeta)(3 - 2\eta)\eta^2 \\ &\quad + (a_r P_i^{s=2}(\zeta) + \dots)(a_t P_i^{s=2}(\eta) + \dots); \quad r, t = 6, 8, \dots, N \\ N_2(\zeta, \eta) &= g_1(\zeta, \eta) + \sum_{n,m=5}^M G_i(\zeta, \eta)(1 - \zeta)\eta(1 - \eta)^2 + (b_{1n} P_n^{s=2}(\zeta) + \dots)(b_{2m} P_m^{s=2}(\eta) \\ &\quad + \dots); \quad n, m = 5, 6, \dots, M \end{aligned} \quad (14)$$

It should be noted that the unknown coefficients of the complementary term of shape function N_1 must be equal, $a_r = a_t$, due to the anti-symmetric deflection of shape function N_1 in both ζ and η directions. In the third step, functions introduced in Equation (14) must produce the entries of SCSM. This can be achieved by,[30]

$$K_{i,j} = \int_0^1 \int_0^1 \Upsilon^T(N_i(\zeta, \eta)) D(\zeta, \eta) \Upsilon(N_j(\zeta, \eta)) d\zeta d\eta \quad (15)$$

The operator Υ describes the strain field of the element, and $D(\zeta, \eta)$ denotes the elastic constant function.[30] Employing the proposed shape functions, Equation (14), into Equation (15), the following equations for entries of stiffness matrix are obtained as follows:

Table 2. Hierarchical polynomials obtained from Equation (11).

$p_5(\xi) = \frac{1}{8}\xi - \frac{1}{4}\xi^2 + \frac{1}{8}\xi^4$	
$p_6(\xi) = \frac{1}{8}\xi - \frac{1}{4}\xi^3 + \frac{1}{8}\xi^5$	
$p_7(\xi) = -\frac{1}{48} + \frac{3}{16}\xi^2 - \frac{5}{16}\xi^4 + \frac{7}{48}\xi^6$	

$$\begin{aligned}
 k_{1,4} + k_{1,7} + 4k_{1,5} - 4k_{1,8} &= 6; \quad 2k_{2,6} - 2k_{2,9} - k_{1,6} + k_{1,9} + v = 0. \\
 k_{2,11} + k_{2,8} - k_{1,8} - 2k_{2,9} &= \frac{4288}{1,091,475} a_6^2 b_{15}^2 b_{26}^2 - \frac{17,152}{1,091,475} b_{12}^2 b_{22}^2 \\
 k_{1,10} + k_{1,7} - 4k_{1,12} - 4k_{1,9} &= 6; \quad k_{3,12} + k_{3,9} + \frac{k_{1,12}}{3} + \frac{k_{1,9}}{3} = 0; \\
 k_{2,11} + k_{2,8} - k_{1,8} - 2k_{2,9} &= -\frac{125}{1225} b_{15}^2 b_{25}^2 + \frac{2944}{72,765} b_{15}^2 b_{26}^2 - \frac{17,152}{1,091,475} b_{16}^2 b_{26}^2 \\
 k_{1,7} - k_{1,6} + 2k_{1,8} - k_{1,9} - 2 + v &= \frac{5888}{72,765} b_{15} b_{25} b_{16} b_{26} + \frac{4288}{1,091,475} a_6^2 b_{16} b_{26} \\
 k_{2,5} + k_{2,8} - \frac{k_{1,5}}{3} - \frac{k_{1,8}}{3} &= -\frac{128}{1225} b_{15}^2 b_{25}^2 + \frac{2944}{72,765} b_{15}^2 b_{26}^2; \\
 k_{1,7} + 2k_{1,8} - 2k_{1,9} &= 2;
 \end{aligned} \tag{16}$$

Ahmadian et al. [25] show minimum conditions for a stiffness matrix to represent Kirchhoff plate stiffness model are as follows:

$$\begin{aligned}
 k_{1,10} + k_{1,7} - 4k_{1,12} - 4k_{1,9} &= 6p^2, \quad k_{1,7} + 2k_{1,8} - 2k_{1,9} = 2, \quad k_{3,12} + k_{3,9} + \frac{k_{1,12}}{3} + \frac{k_{1,9}}{3} = 0, \\
 k_{1,4} + k_{1,7} + 4k_{1,5} - 4k_{1,8} &= \frac{6}{p^2}, \quad k_{3,6} + k_{3,9} - 2k_{2,9} + k_{1,9} = 0, \quad k_{2,11} + k_{2,8} - k_{1,8} - 2k_{2,9} = 0, \\
 k_{2,5} + k_{2,8} - \frac{k_{1,5}}{3} - \frac{k_{1,8}}{3} &= 0, \quad k_{1,7} - k_{1,6} + 2k_{1,8} - k_{1,9} = 2 - v, \quad 2k_{2,6} - 2k_{2,9} - k_{1,6} + k_{1,9} = -v
 \end{aligned} \tag{17}$$

where p and v represent the aspect ratio and Poisson ratio, respectively. Satisfying these conditions ensures the FE discrete differential equations have converging solution to Kirchhoff plate governing equation. Overall, requirements defined by Equations (5)–(7) (16) and (17) provide five independent constraints to be satisfied. Therefore, five unknown coefficients must be considered. Two unknown coefficients are obtained when Equations (5)–(7) and (16) are satisfied. Hence, the following relationship between coefficients must be met as follows:

$$b_{15} = 0; \quad a_6 = 2\sqrt{b_{16}b_{26}} \tag{18}$$

In order to determine the three unknown coefficients, Equation (18) is substituted into Equation (17). Therefore, Equation (17) can be re-written based on three unknown coefficients as follows:

$$\begin{aligned}
 k_{15} &= \frac{17,152}{1,091,475} b_{16}^2 b_{26}^2 - \frac{1}{5}v + \frac{11}{5}, \quad k_{29} = \frac{4288}{1,091,475} b_{16}^2 b_{26}^2 \\
 k_{28} &= \frac{1472}{72,765} b_{16}^2 b_{25}^2 - \frac{1}{15}v - \frac{4288}{1,091,475} b_{16}^2 b_{26}^2 + \frac{2}{5}
 \end{aligned} \tag{19}$$

The remaining three unknown coefficients can be readily determined by equating the Equation (19) with the Equation (20). Equation 20 is obtained from the SCSM [25]:

$$k_{15} = \frac{14}{5}; k_{29} = -\frac{2}{10}; k_{28} = \frac{1}{15} \quad (20)$$

However, it should be mentioned that the values obtained by equating two Equations (19) and (20) are unacceptable because these equations are not independent. For this reason, one may apply a new strategy to determine these three unknowns. This strategy is based on the theorem that two $m \times m$ matrices are similar when they have the same characteristic polynomial and hence eigenvalues. Therefore, here, the eigenvalues of both parametric stiffness matrix and the SCSM must be identical. Indeed, the three unknown coefficients are obtained in such a way that the discrepancy between eigenvalues of both matrices approaches to zero. The objective function which is the norm of discrepancy between eigenvalues of both matrices is defined as follows:

$$\Pi = \left\| \left(\lambda_{4,scsm} - \lambda_{4,par} \right)^2, \left(\lambda_{5,scsm} - \lambda_{5,par} \right)^2, \dots, \left(\lambda_{12,scsm} - \lambda_{12,par} \right)^2 \right\| \quad (21)$$

s.t

$$\lambda_{i,par} > 0; i = 4, 5, \dots, 12$$

where $\lambda_{i,scsm}$ denotes the nonzero eigenvalues of the SCSM, and $\lambda_{i,par}$ represents the nonzero eigenvalues of the parametric stiffness matrix. Here, genetic algorithm (GA) as the global search is taken into account to solve numerically the constraint minimization problem.

3.1. Minimization using genetic algorithm

A GA is a stochastic global search technique based on Darwin's evolution theorem of 'survival of fittest'. [42,43] GA is a powerful approach for a wide range of optimization problems. The method was first inspired by Holland [44] and used by many others as one of the most popular and practical meta-heuristic approaches. In this study, a GA is employed as a global optimizer to find optimal solution of the attempted problem. In order to minimize Equation (21), the following steps need to be considered.

- First, an initial population of chromosomes is randomly generated as a predefined population size.
- Second, each chromosome in the population is evaluated through a predefined fitness function, Equation (21).
- Next, the roulette wheel technique is employed to select parents, and then the crossover and mutation operators are used to produce new offspring (children) from the selected parents, and newly generated offspring are estimated according to fitness function.
- Then, the new generation is chosen and produced from the parents and offspring using the roulette wheel and elitism policy.
- Finally, the pre-described stopping criterion for the algorithm is checked. If the algorithm reaches to a predefined number of iterations, the search process terminates, otherwise the algorithm goes to step 3.

Details of each step are described as follows.

3.1.1. Chromosome representation

A segmented chromosome is developed in order to encode solutions of the problem into chromosome scheme. The initial chromosome is $1 \times n$ matrix which n stands for the number of variables. The initial chromosome is created through a pure random process between -3 and 3 . Each chromosome (population) encodes a solution of the problem. Therefore, based on the GA evolutionary procedure, at the end of GA procedure, good solutions will be obtained (based on population size), that individually represents a shape functions.

3.1.2. Selecting operator

Selecting two individuals (parent) from the current population is performed in the selection operation process. Here, one may employ the roulette wheel selection procedure where the selection probability of each chromosome is proportional to its fitness value. In the proposed algorithm, the selection probability of chromosome i denoted by $p_{selection}(i)$ is stated by Equation (22) where $Ft(i)$ is the fitness of chromosome i [45]:

$$p_{selection}(i) = \frac{1/Ft(i)}{\sum_j 1/Ft(j)} \quad (22)$$

It should be mentioned that the objective function is considered the value associated with a chromosome as the fitness value of that chromosome. Since the objective function of the formulated model is minimization, the reverse of fitness value in Equation (22) is considered to enhance the selection probability of the chromosome with lower fitness.

3.1.3. Crossover operator

In the proposed algorithm, one may employ the crossover operator in order to generate offspring from parents. This is performed in a way that the first and third values of initial population are exchanged between two parents. Therefore, construct the first child code is constructed based on the first value of the first parent and the third value of the second parent, and vice versa, for the second child.

3.1.4. Mutation operator

One may use the mutation operator to bring unexpected changes to the content of a chromosome. Here, the mutation operator is called as a 'swap mutation' where randomly are selected two columns of the initial populations, and then swap their contents.

3.1.5. Reproduction

In this step, one may select the new generation from among the old generation and newly generated offspring. Next, two mechanisms are used, namely elitism policy and roulette wheel in the proposed algorithm to select the new generation. The elitism mechanism empowers the intensification capability of the algorithm, and the roulette mechanism enhances its diversification. One may select the best p_e per cent, a pre-determined per

cent, of the current chromosomes using the elitism policy, and the roulette wheel technique is used to select the rest of new generation.

3.1.6. Stopping criteria

As a stopping criterion to terminate the computation process of the proposed GA, one may simply define the maximum number of iterations.

Using the above strategy, the convergence curve vs. the number of iterations for minimizing the error function, Equation (21), is shown in Figure 3. The following values are obtained for unknown series coefficients as follows:

$$b_{16} = 2.5889; b_{26} = 2.5032; b_{25} = -1.2646; \quad (23)$$

The obtained hierarchal shape functions $N_1(\zeta, \eta)$ and $N_2(\zeta, \eta)$ of the rectangular plate element are depicted in Figures 4 and 5. The other ten shape functions are obtained by rotation of $N_1(\zeta, \eta)$ and $N_2(\zeta, \eta)$ about the axis normal to the element plane as shown in Table 1.

The new consistent mass matrix of thin plate element can be obtained by employing the new shape functions as follows:

$$M = \int_0^1 \int_0^1 N_i^T(\zeta, \eta) \rho(\zeta, \eta) N_j(\zeta, \eta) |J(x, y)| d\zeta d\eta \quad (24)$$

where $\rho(\zeta, \eta)$ is the mass density distribution, and $J(x, y)$ is the Jacobian of the coordinate transformation. Using the new obtained shape functions, plate element formulation can be transformed from local to global coordinate. Indeed, using these shape functions, the superconvergent property of the model can be utilized in global coordinate. In order to transform the element formulation from local to global, the displacement field and geometry of element are mapped using the new obtained shape function and bilinear shape functions, respectively.

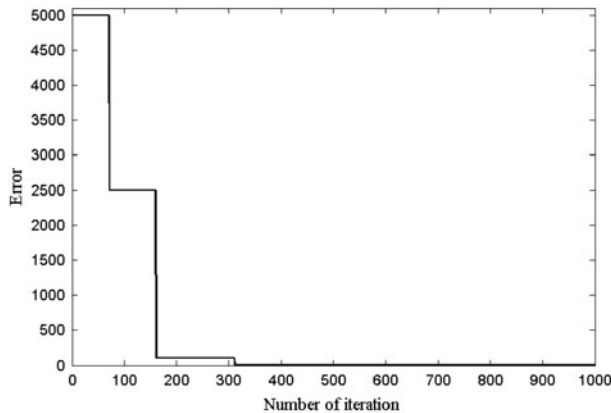


Figure 3. The convergence curve vs. the number of iterations.

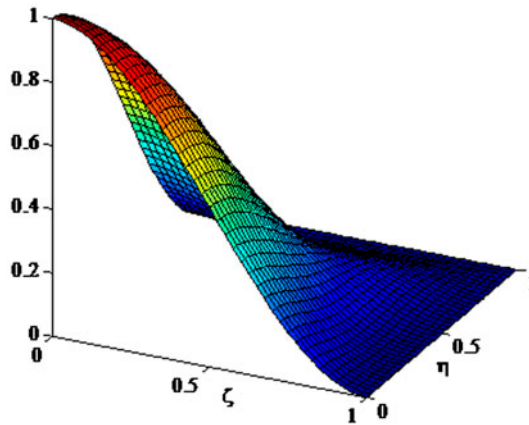


Figure 4. Shape function $N_1(\zeta, \eta)$ of thin plate element.

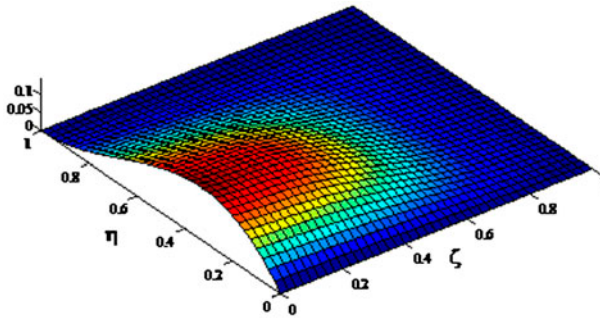


Figure 5. Shape function $N_2(\zeta, \eta)$ of thin plate element.

The numerical performance of the plate element is evaluated in the local and global coordinates using these new shape functions. Indeed, comparisons on the convergence rate for estimating the plate's deflection and its associated eigenvalues are discussed in the next section.

4. Numerical examples

Three numerical examples are used to demonstrate the competence of the model obtained by the proposed shape functions. Here, errors in estimation of static deflection and eigenvalues of the thin plate are compared with the numerical FE results and the analytical solution. MATLAB version 7.4 (R2007a) is utilized for computational calculation programming. The aim of these examples is to numerically illustrate the fact that the new formulation is the most robust model for analysing the static and dynamic plate problems in local coordinates (examples 1 and 2) and in global coordinates (example 3), respectively.

4.1. Example 1: a square clamped-simply supported thin plate

A square plate clamped on two opposite edges and simply supported on the remaining edges subject to a uniformly distributed load and concentrated load separately is modelled using five different formulations including MZC,[8] JWU,[39] ZQC,[38] AFM [25] and the proposed model. The exact non-dimensional solutions are 0.001256 for the case of distribute load and 0.0116 for concentrated load.[46] Figures 6 and 7 demonstrate the errors in the evaluation of the non-dimensional static deflection of the clamped and simply supported plate's mid-node, respectively. Indeed, they show the convergence rate of these models when the number of elements is increased. It is noticeable from Figures 6 and 7, that the convergence rate for the AFM and proposed model is the same, which are superior (much faster) than the MZC, JUV and ZQC models. One may conclude from these examples that the AFM and proposed model are the best formulation to be used in modelling thin plate in local coordinates.

4.2. Example 2: eigenvalues of square clamped thin plate

In the second example, the eigenvalues of a square clamped thin plate with length ' a ' are calculated using MZC, AFM, proposed model and the Rayleigh–Ritz [47] approach. In the proposed model, the mass matrix is defined based on Equation (24); while in AFM model, the mass matrix is obtained by minimizing the error terms with a least squares sense.[25] Here, the solution acquired by Rayleigh–Ritz approach is considered as a reference. Table 3 reports the non-dimensional eigenvalues of a square clamped thin plate for different element sizes using aforementioned models. According to Table 3 results, it can be deduced that the convergence rate of the proposed model is equal to that of AFM model; however, the convergence rate of these models are much faster than MZC model. The accuracy of the proposed model and AFM model is of the order four, while the accuracy of the MZC model is of order two.

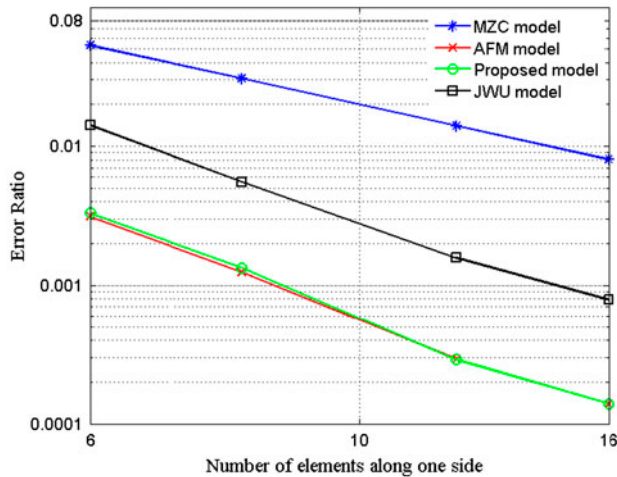


Figure 6. Error in estimation of static deflection of the fully clamped square plate.

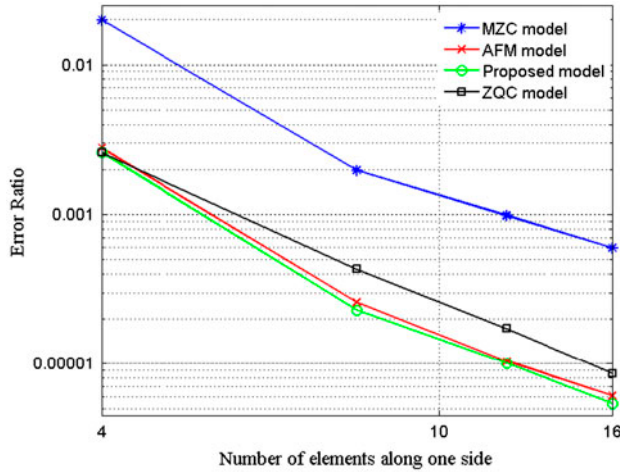


Figure 7. Error in estimation of static deflection of the fully simply supported square plate.

4.3. Example 3: annular thin plate

In the third example, the annular thin plate with $b/a = 0.5$ is considered as depicted in Figure 8. The internal edge of the annular thin plate is fully clamped, and the distributed load is applied at the external edge. Considering the symmetry of the annular thin plate, only a sectorial of the annular thin plate ($b/a = 0.5$, $\varphi = 90^\circ$) is taken into consideration for modelling. The non-dimensional static deflection of node B is 0.458 [48] and has coordinates of $r = 0.75$, $\varphi = 45$. The sectorial of the thin plate is investigated by mapping the square elements into quadrilateral elements as illustrated in Figure 9.

The MZC model and the proposed model are both transformed into a global coordinate. For two models, the geometry is mapped by bilinear shape function, and the displacement fields are mapped using correspond shape functions. Also, the integrals are performed based on Gauss–Legendre quadrature rule. Here, the stiffness matrix of annular thin plate is obtained using 5 Gauss points.

In order to highlight the convergence rate of solutions approximated by different plate element models, the static deflection obtained using the MZC, and the proposed models are shown in Figure 10. Figure 10 shows the errors in the evaluated static deflection of sectorial plate vs. the number of used radial elements on logarithmic scale. In this numerical example, the number of elements in radial and tangential directions is kept fixed at their initial value, whereas the number of elements along each side is increased from 4 to 12. It can be seen from Figure 10, that the proposed model provides more accurate results. The rate of convergence in proposed models is also faster to that of the MZC model. The computational efforts and time elapsed to solve a problem are almost the same for both models, while the proposed model in this study remarkably produces more accurate results.

Table 3. Non-dimensional eigenvalues of square clamped thin plate $\omega d^2 \sqrt{\rho/D}$.

	MZC model			AFM model			Proposed model					
	4 × 4	8 × 8	12 × 12	16 × 16	4 × 4	8 × 8	12 × 12	16 × 16	4 × 4	8 × 8	12 × 12	16 × 16
Rayleigh Ritz [44]	34.31	35.45	35.74	35.84	35.87	35.97	35.98	35.98	35.94	35.97	35.98	35.98
35.98												
73.39	70.03	72.04	72.74	73.01	73.18	73.36	73.39	73.39	73.59	73.37	73.39	73.39
73.39	70.03	72.04	72.74	73.01	73.18	73.36	73.39	73.39	73.59	73.37	73.39	73.39
108.22	98.06	103.71	106.00	106.92	108.02	108.06	108.18	108.20	107.99	108.07	108.18	108.20
131.58	127.58	129.49	130.44	130.90	129.39	131.52	131.57	131.58	131.32	131.64	131.59	131.58
132.20	129.62	130.28	131.16	131.58	130.47	132.13	132.19	132.20	132.93	132.28	132.23	131.22

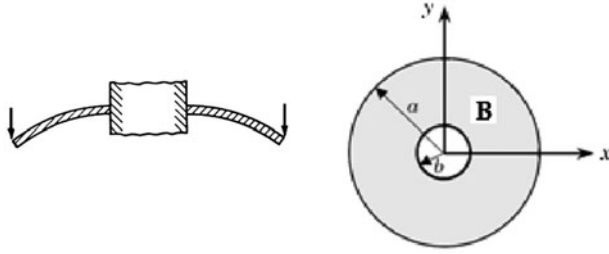


Figure 8. The annular thin plate with load condition.

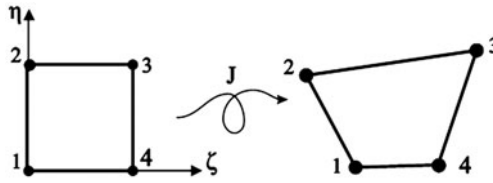


Figure 9. Two-dimensional 'mapping' of the square element.

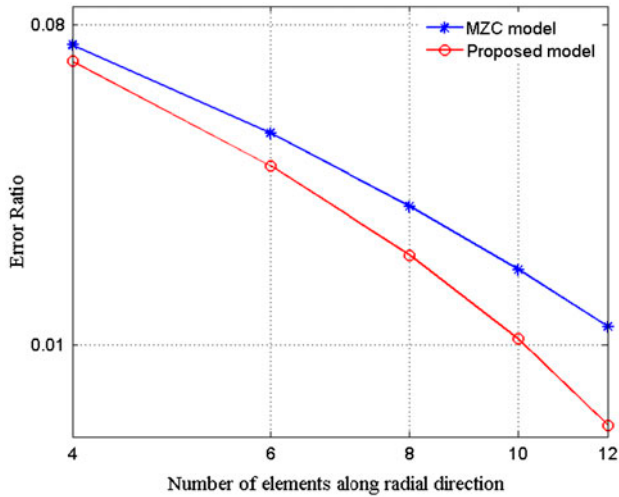


Figure10. Error in estimation of static deflection of the annular thin plate.

5. Conclusion

In this article, an inverse approach is proposed to produce the shape functions associated with the SCSM of plate element. These shape functions are composed of two terms: first term includes the classical shape functions of the plate element satisfying the boundary conditions, and the second term is the hierarchal polynomials sets. The

unknown coefficients of the polynomial are assigned in such a way that the essential conditions of shape functions are satisfied and also regenerate the SCSM of plate element. These new obtained shape functions are then utilized to map the displacement field of the plate element to the global coordinates. Numerical examples show that the new formulation is more accurate than other reported models.

Disclosure statement

No potential conflict of interest was reported by the authors.

References

- [1] Zienkiewicz OC, Taylor RL. The finite element method. 4th ed. New York (NY): McGraw-Hill; 1989.
- [2] Houmat A. A sector elliptic p-element applied to membrane vibrations. *Thin-walled Strut.* 2009;47:172–177.
- [3] Ayad R, Dhatt G, Batoz JL. A new hybrid-mixed variational approach for Reissner–Mindlin plates. The MiSP model. *Int. J. Numer. Methods Eng.* 1998;42:1149–1179.
- [4] Kikuchi F, Ishii K. An improved 4-node quadrilateral plate bending element of the Reissner–Mindlin type. *Comput. Mech.* 1999;23:240–249.
- [5] Zienkiewicz OC, Taylor RT. The finite element method. 4th ed. New York (NY): McGraw-Hill; 1991.
- [6] Allman DJ. A quadrilateral finite element including vertex rotations for plane elasticity analysis. *Int. J. Numer. Methods Eng.* 1988;26:717–730.
- [7] Melosh JR. Basis for derivation of matrices for the direct stiffness method. *AIAA J.* 1963;1:1631–1637.
- [8] Pian THH. Derivation of element stiffness matrices by assumed stress distributions. *AIAA J.* 1964;2:1333–1336.
- [9] Leonard R. Herrmann. Finite element bending analysis for plates. *J. Eng. Mech. Div. ASCE.* 1967;93:13–26.
- [10] Washizu K. Variational method in elasticity and plasticity. 2nd ed. Oxford: Pergamon Press; 1975.
- [11] Zhou YH, Wang JZ, Zheng XJ. Application of wavelet Galerkin FEM to bending of beam and plate structure. *Appl. Math. Mech. English Ed.* 1998;19:745–755. From China.
- [12] Zhou YH, Wang JZ, Zheng XJ. Application of wavelet Galerkin FEM to bending of plate structure. *Acta Mech. Solida Sin.* 1999;12:136–143.
- [13] Han JG, Ren WX, Huang Y. A wavelet-based stochastic finite element method of thin plate bending. *Appl. Math. Model.* 2007;31:181–193.
- [14] Zhou YH, Zhoua J. A modified wavelet approximation of deflections for solving PDEs of beams and square thin plates. *Finite Elem. Anal. Des.* 2008;44:773–783.
- [15] Leung A, Chan J. Fourier p-element for the analysis of beam and plates. *J. Sound Vib.* 1998;212:79–85.
- [16] Argyris JS, Haase M, Mlejnek HP. On an unconventional but natural formation of a stiffness matrix. *Comput. Methods Appl. Mech. Eng.* 1980;22:1–22.
- [17] Bergan PG, Nygård MK. Finite elements with increased freedom in choosing shape functions. *Int. J. Numer. Methods Eng.* 1984;20:643–663.
- [18] Simo C, Rifai MS. A class of mixed assumed strain methods and the method of incompatible modes. *Int. J. Numer. Methods Eng.* 1990;29:1595–1638.

- [19] MacNeal-Schwendler Corp. NASTRAN theoretical manual. Los Angeles (CA): NASA SP-221(01); 1972.
- [20] Kim KI. A review of mass matrices for eigenproblems. *Comput. Strut.* 1993;46:1041–1048.
- [21] Hansson PA, Sandberg G. Mass matrices by minimization of modal errors. *Int. J. Numer. Methods Eng.* 1997;40:4259–4271.
- [22] Fried I, Chavez M. Superaccurate finite element eigenvalue computation. *J. Sound Vib.* 2004;275:415–422.
- [23] Fried I, Leong K. Superaccurate finite element eigenvalues via a Rayleigh quotient correction. *J. Sound Vib.* 2005;288:375–386.
- [24] Stavrinidis C, Clinckemaijlet J, Dubois J. New concepts for finite element mass matrix formulations. *AIAA J.* 1989;27:1249–1255.
- [25] Ahmadian H, Friswell MI, Mottershead JE. Minimization of the discretization error in mass and stiffness formulations by an inverse method. *Int. J. Numer. Methods Eng.* 1998;41:371–387.
- [26] Ahmadian H, Faroughi S. Super-convergent eigenvalue bending plate element. *Inv. Prob. Sci. Eng.* 2010;18:1–18.
- [27] Faroughi S. Development of a new formulation for a beam element with displacement DOF using an inverse method. *Inv. Prob. Sci. Eng.* 2013;28:1–18.
- [28] Ahmadian H, Faroughi S. Shape functions of superconvergent finite element models. *Thin-walled Strut.* 2011;49:1178–1183.
- [29] Faroughi S, Ahmadian H, Ghareghani A. Shape functions associated with super-convergent mass matrix. *Inv. Prob. Sci. Eng.* 2011;14:1–9.
- [30] Faroughi S, Ahmadian H. Shape functions associated with the inverse element formulations. *J. Mech. Eng. Sci. Part C.* 2010;225:304–311.
- [31] Houmat A. Hierarchical finite element analysis of the vibration of membranes. *J. Sound Vib.* 1997;201:465–472.
- [32] Bardell NS. Free vibration analysis of a flat plate using the hierarchical finite element method. *J. Sound Vib.* 1991;151:263–289.
- [33] Taazount M, Zinai A, Bouazzouni A. Large free vibration of thin plates: hierarchic finite element method and asymptotic linearization. *Eur. J. Mech. A Solids* 2009;28:155–165.
- [34] Beslin O, Nicolas J. A hierarchical function set for predicting very high order plate bending modes with any boundary conditions. *J. Sound Vib.* 1997;202:633–655.
- [35] Jie F. P version finite elements in structural dynamics and stability [PhD Thesis]. Hong Kong: Department of Building and Construction, University of Hong Kong; Sep 2010.
- [36] Barrette M, Berry A, Beslin O. Vibration of stiffened plates using hierarchical trigonometric functions. *J. Sound Vib.* 2000;235(5):727–747.
- [37] Bogner FK, Fox LR, Schmit LA. The generation of inter element compatible stiffness and mass matrices by the use of interpolation formulas. *Proceedings of the Conference on Matrix Methods in Structural Mechanics*; 1965, AFIT, Wright-Patterson AF Base, OH. p. 397–443.
- [38] Shi Z, Chen Q. An efficient rectangular plate element. *Sci. China.* 2001;44:145–158.
- [39] Han JG, Ren WX, Huang Y. A spline wavelet finite element formulation of thin plate bending. *Eng. Comput.* 2009;25:319–326.
- [40] Zhu DC. Development of hierarchal finite element method. In: Genki Yagawa, Satya N. Atluri, editors. *Proceedings of the international conference on computational mechanics*; Tokyo: Springer; 1986.
- [41] Bardell NS. The free vibration of skew plates using the hierarchical finite element method. *Comput. Strut.* 1992;45:841–874.
- [42] Goldberg D. *Genetic algorithms in search, optimization, and machine learning*. Reading (MA): Addison-Wesley; 1989.
- [43] Michalewicz Z. *Genetic algorithms + data structures = evolution programs*. Berlin: Springer-Verlag; 1992.

- [44] Holland JH. *Adaptation in natural and artificial systems*. Ann Arbor (MI): University of Michigan Press; 1975.
- [45] Lee KY, Han SN, Roh MI. An improved genetic algorithm for facility layout problems having inner structure walls and passages. *Comput. Operat. Res.* 2003;30:117–138.
- [46] Timoshenko SP, Woinowsky-Krieger S. *Theory of plates and shells*. New York (NY): McGraw-Hill; 1959.
- [47] Vijayakumar K, Ramaiah GK. Analysis of vibration of clamped square plates by the Rayleigh–Ritz method with asymptotic solutions from a modified Bolotin method. *J. Sound Vib.* 1978;56:127–135.
- [48] Timoshenko Stephaen P, Woinowsky-Krieger S. *Theory of plate and shells*. 2nd ed. Singapore: McGraw-Hill International Editions.